Chinese Chemical Letters 37 (2026) 112568

Contents lists available at ScienceDirect

Chinese Chemical Letters

journal homepage: www.elsevier.com/locate/cclet

# White-light organic molecule based on structural regulation of aldehyde–gemdiol equilibrium and its applications in information encryption

Xuerui Song[a], Xi Hu[a], Zhengxing Zeng[a], Ruikang Qin[a], Ting Wang[a], Huan Yang[a,b], Chuanfeng Wang[a,*], Zhouyu Wang[a,c,*], Xiaoqi Yu[a]

[a] Sichuan Provincial Engineering Research Center of Molecular Targeted Diagnostic & Therapeutic Drugs, Department of Chemistry, Xihua University, Chengdu 610039, China
[b] Key Laboratory of High-Performance Scientific Computation, Xihua University, Chengdu 610039, China
[c] Asymmetric Synthesis and Chiral Technology Key Laboratory of Sichuan Province, Chengdu 610039, China

ARTICLE INFO

*Article history:*
Received 12 December 2025
Revised 16 February 2026
Accepted 2 March 2026
Available online 3 March 2026

*Keywords:*
Fluorescent
Organic single molecule
White light
Aldehyde–gemdiol balance
Information encryption

ABSTRACT

White-light organic molecules (WLOMs) exhibit distinct advantages over multi-component systems, such as good reproducibility and high long-term stability. However, the complex synthesis method and the unsatisfactory CIE coordinates hinder their further application. To meet this challenge, a series of novel white-light-emitting single-molecule compounds (BTP-Phs) based on the benzothiazolopyridinone skeleton were rationally designed and synthesized by modulating the donor-acceptor (D-A) structure of the molecules. The study of the structure-spectra relationship indicated that the strong electron-donating ability of the aromatic substituents and the synergistic effect of the extended $\pi$-conjugated system enhanced the intramolecular charge transfer (ICT), which reduces the energy gap of the molecules and favors the long-wavelength emission of BTP-Phs. Notably, ideal white light emission (0.31, 0.34) was achieved through the aldehyde-gemdiol equilibrium in mixed solvents. The emission color could be finely tuned by solvent composition, excitation wavelength and concentration. In addition, a fluorescent ink was developed based on BTP-CHO-OPh as a functional material, which could realize information storage and encryption through QR codes or ASCII binary encoding. This study not only provides valuable design strategies for constructing WLOMs based on aldehyde-geminal diol equilibrium, but also highlights their potential in the field of secure information technology.

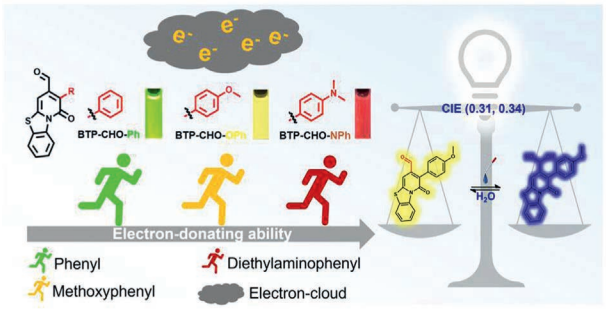
© 2026 Published by Elsevier B.V. on behalf of Chinese Chemical Society and Institute of Materia Medica, Chinese Academy of Medical Sciences.

White-light emitting materials have attracted wide attention due to their potential applications in solid-state lighting, displays, and security technologies [1–7]. White-light emission usually requires simultaneous photon emission in multiple spectral regions within the visible spectrum. However, the realization is limited by Kasha's rule [8,9]. Traditional methods rely on mixing multiple chromophores, such as covalent organic frameworks (COFs) [10–14], nanoparticles [15–17], and hydrogels [18–23]. Although these methods are effective, multi-component systems face challenges such as phase separation, poor reproducibility, and insufficient stability. To overcome this limitation, white-light organic molecules (WLOMs) have become an attractive alternative due to their inherent simplicity and robustness. Researchers have explored various mechanisms to achieve dual or multi-emission, such as intramolecular charge transfer [24], excited-state intramolecular proton transfer (ESIPT) [25–29], conformational isomerism [30–33], and others [27,32,34–40]. In 2022, Xu developed a series of WLOMs and found that they exhibited aggregation-induced delayed fluorescence (AIDF) properties [41]. In 2025, Li reported the design and synthesis of a new type of $\pi$-conjugated fluorescent framework through heterocycle-assisted external C–H alkenylation [42], which exhibit full-color tunable emission with a large Stokes shift. Despite these significant progresses, WLOMs still have limitations such as complex composition and difficult preparation at present. This seriously hinders their application in actual white light materials.

Recently, our group innovatively proposed the use of aldehyde-geminal diol equilibrium based on benzothiazolidine-pyridone sketon to achieve dual emission at the single-molecule level [43]. Unfortunately, this work still encounters the bottleneck of unsat-

* Corresponding authors.
*E-mail addresses:* wangchuanfeng@mail.xhu.edu.cn (C. Wang), zhouyuwang@mail.xhu.edu.cn (Z. Wang).

https://doi.org/10.1016/j.cclet.2026.112568
1001-8417/© 2026 Published by Elsevier B.V. on behalf of Chinese Chemical Society and Institute of Materia Medica, Chinese Academy of Medical Sciences.




**Scheme 1.** The molecular engineering precisely regulates electronic effects to achieve white light emission.

isfactory CIE coordinates. How to realize tunable emission spectra by designing molecular structures and develop novel WLOMs with desirable white light emission is our pursuit. The group containing the phenyl structure has a good electron donor capacity, which can promote the separation of the HOMO from the LUMO. It is beneficial to enhance the ICT, thereby promoting the emission wavelength red shift. Therefore, *N*,*N*-dimethylamine phenyl, phenyl, and phenoxy groups were further introduced on the basis of BTP-CHO to adjust the emission wavelength by different electron donor capacities (Scheme 1). In addition, a well-enhanced donor-acceptor (D-A) structure was constructed in combination with a benzothiazolidine-pyridone backbone. As part of our work, benzothiazolidine-pyridone has also been widely used in the development of fluorescence sensors and photosensitizers [44–48].

In this work, a series of benzothiazole pyridone compounds (BTP-Phs) with the structure as shown in Scheme 1 were rationally designed and successfully synthesized through a simple route. A systematic review was conducted on the structure-spectral relationship. Among the series of compounds, BTP-CHO-OPh exhibits yellow emission (550 nm) in DMSO and blue emission (450 nm) in $H_2O$. Interestingly, when the water fraction ($f_w$) is 30%, BTP-CHO-OPh induces dual emission due to the formation of BTP-GD-OPh (geminal diol form of BTP-CHO-OPh) *via* the aldehyde-geminal diol equilibrium, producing white light (0.31, 0.34). In addition, a fluorescent ink based on BTP-CHO-OPh was developed and successfully applied to binary English encryption and QR code anti-counterfeiting. This study not only expands the universality of the aldehyde-geminal diol equilibrium strategy but also provides a practical platform for organic white-light materials.

The specific synthesis route of the target compounds is shown in Scheme S1 (Supporting information). In this work, benzothiazolopyridinone was used as the skeleton. A series compounds were developed by introducing aromatic substituents with different electron-donating capabilities at the *ortho* position of the aldehyde group. It is expected that the stronger $\pi$-donor effect and hyperconjugation effect of the substituents will extend the conjugation length, enhanced the ICT effect within the molecule, thereby reducing its energy and redshifting the emission of the aldehyde-state molecule, and finally achieving white-light emission. BTP-Phs were purified by column chromatography, and their structures were confirmed by $^1$H NMR, $^{13}$C NMR, and HRMS (Scheme 2)

First, the absorption and emission properties of BTP-Phs in different solvents were studied. As shown in Fig. 1, the absorption wavelengths of the three aryl-substituted compounds in different solvents are mainly in the range of 400–500 nm; the fluorescence emission peaks are mainly in the range of 450–550 nm. Compared with other solvents, the absorption and emission spectra of BTP-Phs in $H_2O$ show significant differences.

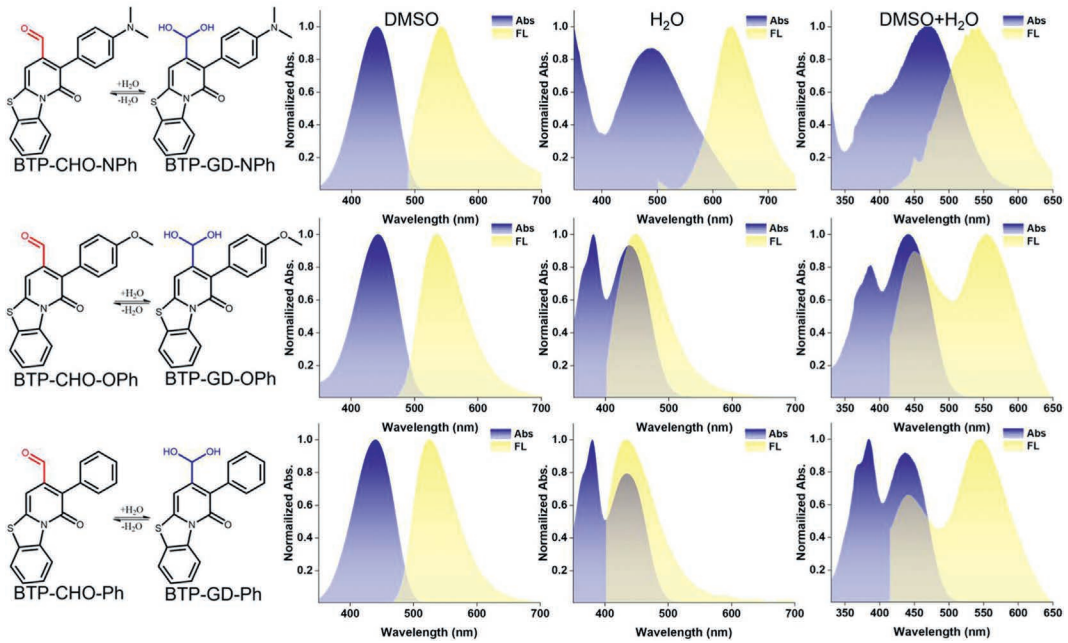
Specifically, the absorption peaks of BTP-Phs in solvents such as acetonitrile (MeCN), *N*,*N*-dimethylformamide (DMF), and DMSO are around 440 nm. It exhibits a maximum absorption redshift of 444 nm in the DMSO. Notably, when water is used as the solvent, the appearance of dual absorption peaks is observed, which may be due to the tautomeric equilibrium of aldehyde-geminal diol. It is speculated that the absorption band blueshifted to 380 nm is attributed to the geminal diol structure in the aldehyde-geminal diol equilibrium; the absorption band at 427 nm is attributed to the aldehyde structure. Correspondingly, the emission peak of BTP-CHO-Ph intense blueshifts from 536 nm to 450 nm.

To further analyze the effect of substituents on the optical properties of the molecules, the optical properties of BTP-Phs in $H_2O$ and DMSO were tested. As shown in Table S1 (Supporting informatioin), the fluorescence emission peaks of BTP-Phs are all in the range of 530–540 nm, indicating that the introduction of aromatic rings successfully redshifts the emission wavelength to yellow light, which is consistent with our expected goal. In addition, analysis of the photophysical properties of BTP-Phs shows that the absorption and emission wavelengths of the compounds increase with the enhancement of the electron-donating ability of the substituents. Furthermore, BTP-CHO-Ph and BTP-CHO-OPh exhibit ultra-high fluorescence quantum yields, but the quantum yield of BTP-NPh shows a sharp decline. This may be due to the freely rotatable *N*,*N*-dimethyl structure in its structure, which induces twisted intramolecular charge transfer (TICT) and significantly enhances the non-radiative decay process.

To study the tunable emission properties of BTP-Phs in DMSO-$H_2O$ mixed solutions, the absorption spectra at different $f_w$ were measured. As shown in Figs. 2A-C, the absorption peak at 450 nm gradually decreases with the increase of $f_w$, while the absorption band at 380 nm increases steadily. This leads to a significant increase in the ratio of the two absorption bands (380 nm and 440 nm). The absorbance decreased significantly when the water content exceeded 80%, which may be due to the poor solubility. With the increase of $f_w$, the emission color of the 5 μmol/L BTP-CHO-OPh solution changes from light yellow to blue (Fig. 2D), and the emission color of the 100 μmol/L solution changes from green to light blue (Fig. 2F). This indicates that the emission from the aldehyde state gradually decreases, while that from the geminal diol state increases, proving that BTP-CHO-OPh can achieve tunable photoluminescence at different $f_w$ values. Interestingly, when $f_w$ reaches 30%, the BTP-CHO-OPh solution exhibits obvious white-light emission (Fig. 2E).

As can be seen from Figs. S7 and S8 (Supporting information), all target compounds show obvious dual absorption peak characteristics in the mixed solvents, which initially indicates that they can form aldehyde-geminal diol equilibrium in the mixed solvents. The substituents alter the electrophilic reactivity of the aldehyde group through electronic effects, thereby shifting the hydration equilibrium (Figs. S14 and S15 in Supporting information). This shift changes the relative proportions of the aldehyde state and its gemdiol state in the solution, and thus affect their fluorescent properties.

To study the tunable properties of BTP-Phs, fluorescence spectroscopy experiments were carried out. As shown in Figs. 3A-C, with the increase of excitation wavelength, the maximum emission peak around 450 nm decreases, while a new emission peak around 550 nm gradually appears. Excitation wavelengths near 350–370 nm preferentially activate the geminal diol state, while longer wavelengths are more likely to excite the aldehyde state, providing an additional means for color regulation. In addition, at low concentrations, the emission of the geminal diol state dominates; with the increase of concentration, the intensity of the aldehyde-state emission (550 nm) of the solution gradually increases, showing dual emission peaks (Figs. S1-S3 in Supporting information), and the solution is observed to gradually change from blue fluorescence to yellow fluorescence.




**Scheme 2.** The aldehyde-geminal diol balance of BTP-Phs, and them spectral property.

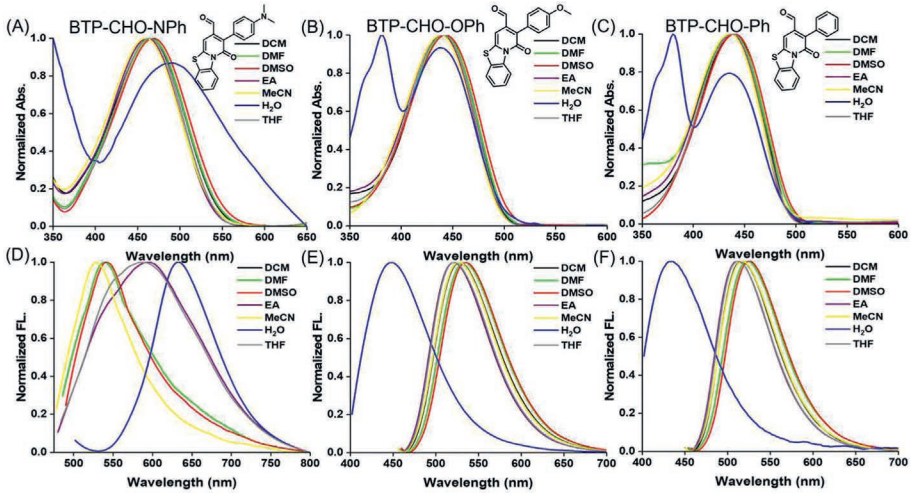



**Fig. 1.** Absorption and fluorescence emission spectra of BTP-NPh (A, D), BTP-CHO-OPh (B, E) and BTP-Ph (C, F) in different solvents.

Surprisingly, during the adjustment of the emission spectrum, when the solution concentration is 20 μmol/L and the excitation wavelength is 395 nm, BTP-CHO-OPh achieves ideal International Commission on Illumination (CIE) chromaticity coordinates of (0.31, 0.34) (Fig. 3E), which is very close to the standard white light (0.33, 0.33). This is a significant improvement compared with the BTP-CHO system, which can only achieve blue-green emission.

Under different excitation wavelengths and concentrations, the CIE coordinates show good linearity (Figs. S4-S6 in Supporting information). Blue light emission can be achieved by using short-wavelength excitation or reducing the concentration, while tunable yellow light emission can be achieved with longer excitation wavelengths or higher concentrations. These results indicate that the tunable multi-color emission of BTP-Phs can be effectively achieved by precisely controlling the excitation wavelength and concentration.

To evaluate the stability of the intrinsic aldehyde-geminal diol equilibrium in the test system, time-dependent experiments were carried out on BTP-CHO-OPh (Figs. 3G-I). At different concentrations, the absorption intensity at around 440 nm decreases rapidly, while the absorption band at 380 nm increases correspondingly, reached a stable level within 120 min, and continued to be stable for 96 h. The results show that BTP-CHO-OPh has good stability in the mixed solution ($f_w = 30\,\%$), which is not affected by concentration changes.

To further verify that the tunable luminescent properties of the above target compounds in the mixed solvent are achieved through the intrinsic aldehyde-geminal diol equilibrium, NMR experiments were performed (Fig. S23 in Supporting information). As shown in the Fig. 4A, markedly enhanced single peak at 5.4 ppm and 7.13 ppm were observed for BTP-CHO-OPh in a mixed solvent of DMSO and water, which is consistent with $H_a$' and $H_b$' in the amidoediol structure. Besides, both BTP-CHO-OPh and corresponding geminal diol structure (BTP-GD-OPh) can be observed in the HRMS (Fig. 4B). This directly indicates that the aldehyde and geminal diol structure coexist in the mixed solution, and the aldehyde-geminal diol equilibrium does exist.

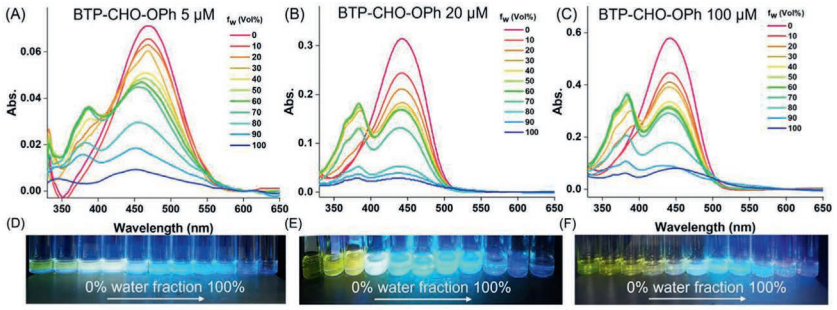



**Fig. 2.** Absorption spectra and fluorescent pictures of BTP-CHO-OPh in 5 μmol/L (A, D), 20 μmol/L (B, E) and 100 μmol/L (C, F) under different $f_w$. The pictures were acquired under 365 nm UV illumination.

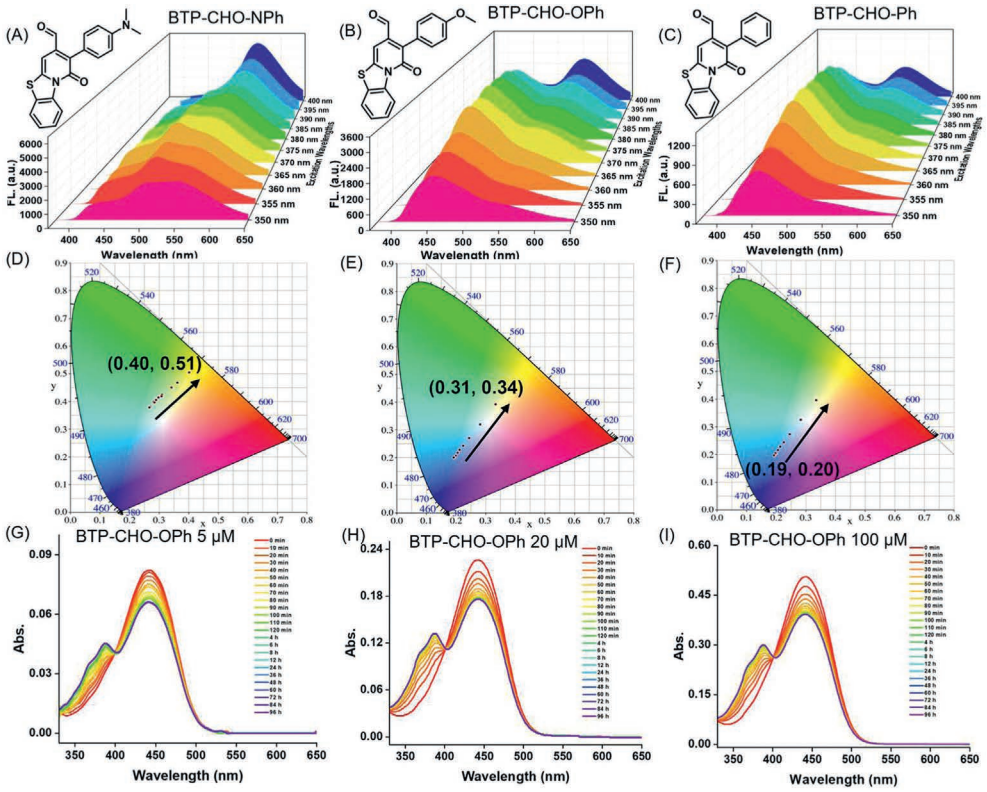



**Fig. 3.** Fluorescence emission spectra and CIE coordinate diagram of 20 μmol/L BTP-CHO-Ph (A, D), BTP-CHO-OPh (B, E) and BTP-CHO-NPh (C, F) with different excitation wavelength. Time-dependent absorption spectra of BTP-CHO-OPh in 5 μmol/L (G), 20 μmol/L (H) and 100 μmol/L (I).

To further analyze the relationship between the multi-color emission properties and structure of BTP-Phs, density functional theory (DFT) calculations were performed on the molecular structure using the Gaussian 09 program (Fig. S25 in Supporting information). The B3LYP/6–31G(d,p) all-electron basis set was used for structural optimization, and all calculation results were visualized using Multiwfn and VMD programs [49–51]. Due to the electron-withdrawing property of the aldehyde group, a shift in the electron cloud distribution of the HOMO and LUMO in BTP-CHO-OPh was observed (Fig. 4C). In contrast, the electron distribution in BTP-GD-OPh is more uniform. Furthermore, according to DFT calculations, the energy gap of BTP-GD-OPh increased by 0.83 eV compared to BTP-CHO-OPh. This is highly consistent with the blue shift observed in the spectroscopic experiments.

The above results prove that the molecular design concept of regulating the emission wavelength of the aldehyde state through the electronic effect of substituents is successful, and also highlight the unique advantages of the benzothiazolopyridinone skeleton in realizing single-molecule tunable white-light emission. It provides a reasonable design idea for expanding the range of emission spectra.

In the current era of information explosion, anti-counterfeiting technology has become particularly important. Fluorescent materials used for information storage and anti-counterfeiting have attracted wide attention [52]. ASCII (American Standard Code for Information Interchange) is the most commonly used and universal single-byte encoding system nowadays. Considering the different fluorescent properties of BTP-CHO-OPh caused by different ratios of water and DMSO, Ink A (DMSO with 20 % water content) and Ink B (DMSO without water content) were selected to design digital encryption patterns based on ASCII encoding, which were successfully constructed through the same "lightning" pattern and different arrangement methods (Fig. 5).

The "lightning" pattern drawn by 7 μL Ink A and Ink B are difficult to distinguish due to their similar color, under 365 UV light or sunlight. The real information cannot be read correctly. After the pattern was smeared with 3 μL water, under 365 nm irradiation, the "lightning" pattern drawn by Ink A appears blue and is set as

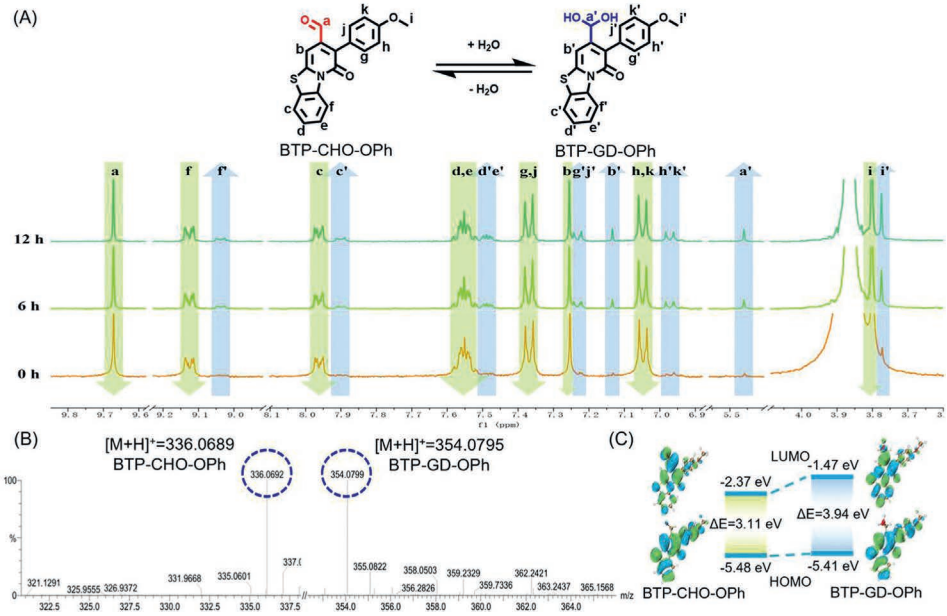



**Fig. 4.** $^{1}$H NMR titration (A), HRMS (B) and DFT (C) experiments of BTP-CHO-OPh.

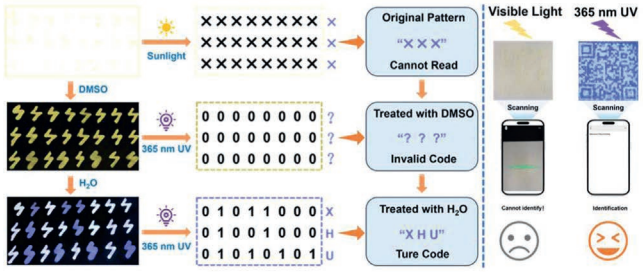



**Fig. 5.** The anti-counterfeiting application based on ASCII encoding of BTP-CHO-OPh ink (left). The encryption application based on QR code of BTP-CHO-OPh ink (right).

"1", while the "lightning" pattern drawn by Ink B appears white and is set as "0". Taking the first row as an example, "01011000" can be read, thus obtaining the encrypted code of the first group of arrangements. By comparing with the standard decryption table (Fig. S28 in Supporting information), the three groups of arrangement codes were finally decoded into "XHU".

Compared with one-dimensional codes, QR codes have many advantages in various fields such as data storage, online payment, and high technology [18]. Hering, the QR code pattern was printed on non-fluorescent paper by BTP-CHO-OPh ink (DMSO/$H_2O$ = 7/3) (Fig. 5). No clear QR code pattern could be displayed under daylight, but it could be clearly observed under UV light. In addition, the QR code could be identified by the scanning function of a smartphone, and the stored encrypted information was successfully read: "Welcome to Xihua University". This indicates that this dual encryption strategy further improves the anti-counterfeiting function.

In summary, this study expands the strategy for single-molecule white-light emission based on the aldehyde-geminal diol equilibrium by introducing electron-donating aromatic substituents into benzothiazolopyridinone skeleton. This design redshifts the emission of the aldehyde state to the yellow region, realizing complementary blue-yellow dual emission and ideal white-light generation (CIE chromaticity coordinates = (0.31, 0.34)). Mechanism studies verify the coexistence and equilibrium of the aldehyde/geminal diol states, and confirms the universality of substituent-regulation. In addition, QR code and ASCII binary encryption demonstrations were successfully realized based on BTP-CHO-OPh ink. This study not only provides a reasonable molecular design idea for WLOMs but also opens up new opportunities for multi-functional fluorescent materials in the field of information security.

## Declaration of competing interest

We declare that we do not have any commercial or associative interest that represents a conflict of interest in connection with the work submitted.

## CRediT authorship contribution statement

**Xuerui Song:** Writing – review & editing, Writing – original draft, Investigation, Formal analysis, Data curation. **Xi Hu:** Formal analysis. **Zhengxing Zeng:** Resources. **Ruikang Qin:** Supervision. **Ting Wang:** Validation. **Huan Yang:** Resources. **Chuanfeng Wang:** Writing – review & editing. **Zhouyu Wang:** Visualization. **Xiaoqi Yu:** Writing – review & editing.

## Acknowledgments

This work was financially supported by the Sichuan Science and Technology Program (Nos. 2023NSFSC1977 and 2022ZYD0048), the Science and Technology Innovation Competition Project for Postgraduate Students, Xihua University (No. YK20240176).

## Supplementary materials

Supplementary material associated with this article can be found, in the online version, at doi:10.1016/j.cclet.2026.112568.

## References

[1] M.Y. Chen, Y. Zhao, L.J. Yan, et al., Angew. Chem. Int. Ed. 56 (2017) 722–727.
[2] G.M. Farinola, R. Ragni, Chem. Soc. Rev. 40 (2011) 3467–3482.
[3] M.C. Gather, A. Köhnen, A. Falcou, et al., Adv. Funct. Mater. 17 (2007) 191–200.
[4] J. Kido, M. Kimura, K. Nagai, Science 267 (1995) 1332–1334.
[5] S. Reineke, F. Lindner, G. Schwartz, et al., Nature 459 (2009) 234–238.
[6] S. Santhosh Babu, J. Aimi, H. Ozawa, et al., Angew. Chem. Int. Ed. 51 (2012) 3391–3395.

[7] C. Vijayakumar, V.K. Praveen, A. Ajayaghosh, Adv. Mater. 21 (2009) 2059–2063.
[8] M. Kasha, Discuss. Faraday Soc. 9 (1950) 14–19.
[9] T. Sun, J.X. Zhang, J. Zhang, et al., J. Am. Chem. Soc. 147 (2025) 39879–39889.
[10] J. Liu, C. Gong, J. Qian, et al., Chin. Chem. Lett. 37 (2026) 111522.
[11] P.T. Furuta, L. Deng, S. Garon, et al., J. Am. Chem. Soc. 126 (2004) 15388–15389.
[12] S. Shinde, S.K. Asha, Macromolecules 49 (2016) 8134–8145.
[13] H. Wu, L. Ying, W. Yang, et al., Chem. Soc. Rev. 38 (2009) 3391–3400.
[14] H. Gao, M. Wang, Y. Mao, et al., Adv. Mater. 35 (2023) 2300616.
[15] A. Layek, P.C. Stanish, V. Chirmanov, et al., Chem. Mater. 27 (2015) 1021–1030.
[16] J. Malinge, C. Allain, A. Brosseau, et al., Angew. Chem. Int. Ed. 51 (2012) 8534-8437.
[17] J. Xiang, S.L. Li, Z.B. Sun, et al., Adv. Opt. Mater. 9 (2021) 2100675.
[18] D. Guo, X. Le, H. Shang, et al., Chin. Chem. Lett. 34 (2023) 108347.
[19] L. Shi, K. Li, L.L. Li, et al., Chem. Sci. 9 (2018) 8969–8974.
[20] D.S. Tu, P. Leong, S. Guo, et al., Angew. Chem. Int. Ed. 56 (2017) 11370–11374.
[21] Q.Y. Yang, J.M. Lehn, Angew. Chem. Int. Ed. 53 (2014) 4572–4577.
[22] J. Zhang, P. Alam, S. Zhang, et al., Nat. Commun. 13 (2022) 3492.
[23] W.J. Chi, Q.L. Qiao, R. Lee, et al., Angew. Chem. Int. Ed. 58 (2019) 7073–7077.
[24] Z. Chen, C.L. Ho, L.Q. Wang, et al., Adv. Mater. 32 (2020) 1903269.
[25] Z. Wang, J.T. Mo, J.J. Pan, et al., Adv. Funct. Mater. 33 (2023) 2300021.
[26] D.F. Li, W.D. Hu, J. Wang, et al., Chem. Sci. 9 (2018) 5709–5715.
[27] M. Li, Z. Li, X. Peng, et al., Angew. Chem. Int. Ed. 64 (2025) 202420474.
[28] Q. Huang, Q. Guo, J.B. Lan, et al., Mater. Horiz. 8 (2021) 1499–1508.
[29] O. Kotova, S. Comby, C. Lincheneau, et al., Chem. Sci. 8 (2017) 3419–3426.
[30] S. Park, J.E. Kwon, S.H. Kim, et al., J. Am. Chem. Soc. 131 (2009) 14043–14049.
[31] K.C. Tang, M.J. Chang, T.Y. Lin, et al., J. Am. Chem. Soc. 133 (2011) 17738–17745.
[32] B.W. Li, Z.Y. Li, F.Y. Guo, et al., ACS Appl. Mater. Interfaces 12 (2020) 14233–14243.
[33] P. Zhao, W.C. Guo, M. Li, et al., Angew. Chem. Int. Ed. 63 (2024) e202409020.
[34] P.L. Lu, K. Li, L. Shi, et al., Mater. Adv. 1 (2020) 61.
[35] M. Song, W. Zhou, J. Wang, et al., J. Rare Earths 43 (2025) 2357–2367.
[36] J. Liu, T. He, Z.L. Gong, et al., Adv. Optical Mater. 12 (2024) 2302486.
[37] X. Li, L. Liu, L. Jia, et al., Nat. Commun. 16 (2025) 467.
[38] Q. Li, Y. Wu, J. Cao, et al., Angew. Chem. Int. Ed. 61 (2022) e202202381.
[39] L. Volyniuk, D. Gudeika, A.A. Panchenko, et al., ACS Sustain. Chem. Eng. 11 (2023) 16914–16925.
[40] F.T. Liu, H. Liu, Y.C. Chen, et al., CCS Chem. 7 (2025) 3172–3184.
[41] Y. Zheng, L. Zuo, L. Zhang, et al., Chin. Chem. Lett. 33 (2022) 4536–4540.
[42] R. Hu, K. Wang, J. Liu, et al., Chin. Chem. Lett. 36 (2025) 110113.
[43] Z.X. Zeng, X.R. Song, X. Hu, et al., Adv. Funct. Mater. 35 (2025) 2504033.
[44] N. Wang, Y.M. Zhang, Z.X. Zeng, et al., Food Chem. 489 (2025) 144930.
[45] Z.X. Zeng, N. Wang, Y.M. Zhang, et al., Chem. Commun. 61 (2025) 13948–13951.
[46] S.Y. Wu, Z.C. Ban, H. Tang, et al., Chem. Commun. 61 (2025) 10574–10577.
[47] Z.C. Ban, N. Ma, H. Tang, et al., Org. Chem. Front. 12 (2025) 6040–6046.
[48] Q. Zhou, S.Q. Wang, X.Y. Ran, et al., Chin. Chem. Lett. 34 (2023) 107922.
[49] T. Lu, J. Chem. Phys. 161 (2024) 082503.
[50] T. Lu, F.W. Chen, J. Comput. Chem. 33 (2012) 580–592.
[51] W. Humphrey, A. Dalke, K. Schulten, J. Mol. Graph. 14 (1996) 33–38.
[52] H. Wang, Y. Tian, T. Wu, et al., Chin. Chem. Lett. 36 (2025) 110509.